*Journal of Applied Research in Water and Wastewater 11(2019) 45-50*

Journal of
Applied Research in Water and Wastewater

Journal homepage: www.arww.razi.ac.ir

**Original paper**

# Plackett–Burman experimental design for the removal of diazinon pesticide from aqueous system by magnetic bentonite nanocomposites

**Somayeh Heydari*, Leili Zare, Hamideh Ghiassi**

*Department of Chemistry, Faculty of Agriculture and Animal Science, Torbat-e jam University, Torbat-e jam, Iran.*

**ARTICLE INFO**

**Article history:**
Received 9 February 2019
Received in revised form 27 March 2019
Accepted 15 April 2019

**Keywords:**
Magnetic bentonite nanocomposites
Diazinon removal
Aqueous system
Plackett–Burman design

**ABSTRACT**

The present study demonstrates the effective removal of diazinon pesticide from aqueous solutions by means of magnetic bentonite nanocomposite. The product was characterized by advanced techniques like scanning electron microscope (SEM), energy dispersive X-ray spectroscopy (EDX) and infrared spectroscopy (IR). Operational parameters affecting the removal efficiency, including the pH level, contact time, agitation speed and adsorbent dose, were screened through Plackett-Burmann design to determine the significant factors. Then, significant parameters, including the pH level and adsorbent dose, were further optimized using Central Composite design to predict optimum removal conditions. Under the optimal conditions, the maximum adsorption capacity of the nanocomposite for diazinon was found to be 92.50 %. The kinetic of pesticide sorption and equilibrium studies were performed. The experimental data could be well fitted to the Freundlich model. The magnetic bentonite nanocomposite was successfully applied for the uptake of diazinon from industrial wastewater and groundwater samples and separated easily by means of magnetic separation.



## 1. Introduction

Diazinon [O, O-diethyl O-(2-isopropyl-4-methyl-6-pyrimidyl) phosphorothioate] (Fig. 1) is one of the most generally used pesticides in agriculture. This nonselective organophosphorus insecticide is used in the many agricultural areas as an urban pest control (Sogorb et al. 2002; Raushel. 2002). As a result of its widespread application, the residue of this insecticide in environment such as water may be hazardous to human and animal health. Therefore, sensitive and efficient water treatment methods are required for removal of Diazinon.

The adsorption technique is one of the most effective methods for removal of pesticides, which has the characteristics of high selectivity and efficiency, flexibility, ease of operation, and designability (Amer et al. 2010). Furthermore, it does not result in the formation of harmful substances like chemical oxidation. The adsorption of diazinon has been examined using natural and synthetic materials such as activated carbons (Hassan et al. 2017; Moussavi et al. 2013), clay minerals (Kabwadza-Corner et al. 2014), and different types biosorbents (Ehrampoush et al. 2017; Yeddou Mezenner et al. 2017). However, in order to improve performance of adsorption, the design of adsorbents with desirable properties such as high selectivity and capacity, fast sorption kinetics and increased mechanical strength, is necessary.

Bentonite is a natural clay containing montmorillonite as a major constituent. This material is one of the promising adsorbents for removing diazinon from water samples as due to its good adsorption capability, low-cost, availability, and eco-friendly (Turabik et al. 2013). Recently, the performance of bentonite has been optimized using different methods. Removing of phosphate species by a new type of bentonite-alum adsorbent was proposed by Mahadevan et al. (2018). The bentonite-alum system with high performance has been used to treat river water streams. Huang et al. (2017) synthesized the organobentonite by modification of bentonite with cetyl trimethyl ammonium bromide (CTAB). Adsorption performance measurement indicated that the organobentonite is an effective adsorbent for removal of Rhodamine B (RhB) and Acid Red 1. Martinez et al. (2017) demonstrated the capability of polymeric Al-modified bentonite to coat the ceramic substrates. In this study, with the help of characterization methods, densification and mullite development of modified bentonite by thermal treatment up to 1200 °C was studied.

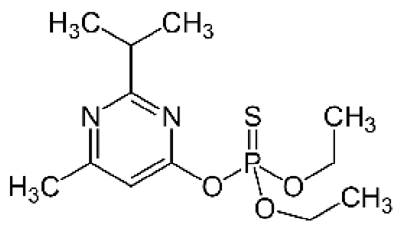


**Fig. 1.** The chemical structure of diazinon.

The coating of bentonite with nano-sized material is one of the most widely used methods for its novel application owing to excellent sorption capacities and high surface area (Lou et al. 2015). Pandey et al. (2017) reviewed the recent advancements in the synthesis of nanocomposites containing bentonite and their applications to remove a variety of inorganic contaminants from water samples. Motawie et al. (2014) synthesized the nano-bentonites as nano-filler using four different types of surfactants, namely hexadecyl trimethyl ammonium bromide (HTAB), 3-aminopropyltriethoxysilane (Silane), octadecylamine (ODA) and dodecylamine (DDA). The production of nano-bentonite and its effects on mutation process in the strains of Salmonella typhimurium are studied by Degtyareva et al. (2016). The study of antimutagenic potential of nano-bentonite reveals that it possesses a moderate inhibitory effect on mutagenesis caused by mitomycin C, 2, 4-dinitrophenylhydrazine, and ethyl methanesulphonate, but does not inhibit genotoxic potential of hydrogen peroxide. Bama and Sundrarajan (2017) synthesized the Ag/$TiO_2$/bentonite nanocomposite

[*]Corresponding author Email: so_heydari_83@yahoo.com

as an antibacterial agent against Staphylococcus aureus (S. aureus) and Escherichia coli (E. coli). Recently, magnetic separation method has attracted much interest in environmental engineering (Mehdinia et al. 2017; Luo et al. 2016). It is expected that the magnetic bentonite with abundant active sites is of great interest because it is quick and can greatly facilitate the separation method. Jiang et al. (2018) synthesized bentonite–$Fe_3O_4$–$MnO_2$ composite for the removal of Cd (II) from aqueous media by effective magnetic separation. Optimization of the variables involved in the process can be performed in order to obtain higher sensitivity and precision, minimum time and materials consumption, and maximum yield. Traditionally, optimization of adsorption studies is achieved by monitoring the influence of one factor at a time (OFAT). The conventional methods do not involve the interaction between factors. In addition, it requires a large number of experiments to be performed each time (Polo et al. 2005). Therefore, the design of experiment methods (DOE) that provides a better understanding of the interaction between factors and reduces the total number of experiments are increasingly preferred (Czitrom. 1999). One of the efficient statistical techniques which is used excessively to screen the important factors is Plackett–Burman designs (PBDs) (Shah et al. 2012). The optimum value of the significant variables and the interactions of these variables are analyzed by a standard response surface methodology (RSM) called central composite design (CCD) (Sousa et al. 2006).

The main objective of this study is to optimize the adsorption performance of magnetic bentonite nanocomposites for the removal of diazinon pesticide from aqueous solution using PBD and employing a central composite design experimental. The isotherm models of Freundlich, Langmuir and Dubinin–Radushkevich were used for the equilibrium studies. Moreover, the kinetic studies were performed as well.

## 2. Materials and methods

### 2.1. Materials

The natural Na-bentonite used for this study was purchased from Vivan (Qaen, Iran). Ferric chloride ($FeCl_3$), Ferro chloride ($FeCl_2$), ammonia ($NH_4OH$, 25 %), hydrochloric acid and sodium hydroxide were obtained from Merck (Germany). Diazinon was purchased from Sigma–Aldrich (Germany) and used without further purification. Diazinon stock solutions (1000 mg/L) were prepared by dissolving diazinon in distilled water. The working solutions were prepared daily by diluting the stock solution to the required experimental concentration.

### 2.2. Synthesis of adsorbent and characterization

To obtain pure bentonite, bentonite was washed several times with distilled water. Then, the bentonite was treated with 1 M HCl and washed again with distilled water. Thereafter, it was dried at 50 °C for 24 h. Then, the dried bentonite was milled and kept in air tight polyethylene container for coating by $Fe_3O_4$ prior to adsorption experiments. In a typical synthesis of $Fe_3O_4$– bentonite nanocomposite, 2 g of $FeCl_2 \cdot 4H_2O$ and 5.2 g of $FeCl_3 \cdot 6H_2O$ were dissolved in 50 mL of distilled water under vigorous stirring at 80 °C. Thereafter, 200 mL of 25 % ammonium hydroxide solution was slowly added to the solution. 3 g of previously prepared bentonite was added to the solution under constant stirring and the reaction was continued for 3 h. The coated bentonite particles were separated by a magnet and washed several times using ultrapure water and dried at 50 ˚C for 24 h. The reactions that occur in the preparation of $Fe_3O_4$–bentonite nanocomposite are shown in following equations:

$$FeCl_2.4H_2O + 2FeCl_3.6H_2O + 8NH_4OH \rightarrow Fe_3O_4 + 8\ NH_4Cl + 14H_2O$$

$$Fe_3O_4 + \text{bentonite} + 14H_2O \rightarrow Fe_3O_4 - \text{bentonite}$$

The surface morphology of the adsorbent was observed with scanning electron microscopy (SEM) images (SEM, TESCAN Mira3) with accelerating voltage of 15 Kv equipped with an energy dispersive X-ray analysis system. Fourier transformed infrared (FTIR) spectrum of $Fe_3O_4$– bentonite sample within the range of 400–4000 $cm^{-1}$ was recorded on Perkin Elmer 1750 FTIR Spectrophotometer. FTIR analysis was performed in order to identify functional groups on the adsorbent surface (Sulaymon et al. 2014).

### 2.3. Batch adsorption experiments

Batch studies were conducted by weighting 0.04 g adsorbent and added into 10 mL beaker. After 3 mL of diazinon solution with different concentrations in pH of 2 was added into sorbent-containing beaker, the mixture was stirred using rotary shaker at 500 rpm for 30 min and then the sample solution was separated using a magnet. The amount of remained diazinon in the solution was determined by measurement of optical density with a double-beam spectrophotometer (Photonix Ar 2017, UV- Vis Array) with 1 nm resolution and optical length of 1 cm at $\lambda_{max}$ of 253 nm. The adsorption was calculated using the following formula:

$$q_e = \frac{(C_0 - C_e)\ V}{W} \tag{1}$$

where, $q_e$ (mg/g) is the equilibrium adsorption capacity, $C_o$ is the initial concentration of diazinon, $C_e$ is the diazinon concentration at equilibrium (mg/L) which is obtained from the equation: $C_e = C_o\ A_2/A_1$, ($A_1$ is the initial adsorption of diazinon solution and $A_2$ is the adsorption of diazinon solution after addition of adsorbent), V is the volume of solution (L) and W is the weight of adsorbent (g)

### 2.4. Experimental design

In this study, a Plackett–Burman design with twelve experiments was applied in order to evaluate the effect of significant factors including the pH level, contact time, agitation speed and adsorbent dose on the adsorption of diazinon from water samples. Each independent variable was assessed at two levels, high and low, which were determined by (+) and (−), respectively. The variables and level of each variable is depicted in Table 1. In this study, 12 runs were applied to assess significance of four factors. To insure the reliability of the results, each experiment was repeated 3 times and results were shown in Table 2. The results were visualized using the Pareto chart. By plotting all the results of the experiments on a Pareto chart, it is easier to evaluate the importance of the significant factors. The analysis of variance (ANOVA) was applied to study the experimental results at 95 % confidence level (p-value < 0.05) and results were shown in Table 3.
MINITAB software (version17, Minitab Inc., USA) was applied for the experimental design and statistical treatment of results.

**Table 1.** Factors and levels used in Plackett–Burman design matrix.

| Variable Code | Variable | Low (-) | High (+) |
|---|---|---|---|
| A | pH | 3 | 7 |
| B | Amount of sorbent(mg/ml) | 2 | 5 |
| C | Contact time (min) | 5 | 30 |
| D | Agitation speed | 200 | 500 |

**Table 2.** The results of Plackett-Burman design matrix.

| Run No. | A | B | C | D | Absorbance |
|---|---|---|---|---|---|
| 1 | 7 | 0.02 | 5 | 500 | 0.90 |
| 2 | 7 | 0.05 | 30 | 200 | 0.51 |
| 3 | 3 | 0.05 | 5 | 500 | 0.31 |
| 4 | 7 | 0.02 | 30 | 500 | 0.72 |
| 5 | 7 | 0.05 | 5 | 200 | 0.81 |
| 6 | 7 | 0.05 | 5 | 500 | 0.53 |
| 7 | 3 | 0.05 | 30 | 500 | 0.31 |
| 8 | 3 | 0.02 | 30 | 500 | 0.33 |
| 9 | 3 | 0.02 | 30 | 200 | 0.41 |
| 10 | 7 | 0.02 | 5 | 200 | 0.72 |
| 11 | 3 | 0.05 | 5 | 200 | 0.31 |
| 12 | 3 | 0.02 | 5 | 200 | 0.45 |

### 2.5. Adsorption isotherm studies

In order to understand the interactive behavior between the adsorbate and absorbent, isothermal studies are carried out for the adsorption of diazinon. Langmuir and Freundlich isotherms are applied and presented as equations 2 and 3, respectively.

$$C_e/q_e = 1/bq_m + C_e/q_m \tag{2}$$

$$q_e = K_f\, C_e^{1/n} \tag{3}$$

where, $q_m$ is the maximum adsorption extent of pollutant adsorbed (mg/g), b is the Langmuir adsorption constant. $K_f$ and 1/n are the constants of Freudlich model dealing with adsorption capacity of the adsorbent and intensity, respectively. Langmuir model explains monolayer adsorption. Fig. 6 a and b shows the adsorption isotherm of diazinon, and the parameters of each model are given in Table 6. The Dubinin –Radushkevich model (equation 4) is generally used to express



Please cite this article as: S. Heydari, L. Zare, H. Ghiassi, Plackett–Burman experimental design for the removal of diazinon pesticide from aqueous system by magnetic bentonite nanocomposites, Journal of Applied Research in Water and Wastewater, 6 (1), 2019, 45-50.

the nature of adsorption as physically and chemically (Ahmed et al. 2013).

$$Lnq_e=\ln(q_m)-K\varepsilon^2 \qquad (4)$$

where, $q_e$ is the equilibrium adsorption capacity, K is a constant related to the mean energy of adsorption, and ε is the polanyi potential which is described as follows:

$$\varepsilon = RT\ln(1+1/C_e) \qquad (5)$$

In Dubinin–Radushkevich isotherm, the mean free energy, E (Kj/mol), shows the mechanism which sorption takes place and defined by equation 6.

$$E=1/\sqrt{2\varepsilon} \qquad (6)$$

Adsorption kinetics investigation are performed to determine the rate controlling step during the adsorption. Kinetic experiments based on pseudo-first-order model represented by equation 7 (Lagergren. 1898).

$$\log(q_e - q_t) = \log q_e - k_1 t/2.303 \qquad (7)$$

where, $q_e$ and $q_t$ denote the amounts of dye adsorbed on sorbent at equilibrium and time t (min), respectively. $k_1$, $q_e$ and correlation coefficient $R^2$ values are presented in Table 7 and Fig. 7a and b. Adsorption kinetic based on second order model is as follows (Ho et al. 1998).

$$t/q_t = 1/k_2 q_e^{\,2} + t/q_e \qquad (8)$$

where, $k_2$ is pseudo-second-order rate constant of adsorption.

**Table 3.** The ANOVA results of the model for diazinon removal.

| Source | Sum of squares | Degree of freedom | Mean square | F-value | P-value | |
|---|---|---|---|---|---|---|
| Model | 0.073333 | 3 | 0.024444 | 5.88 | 0.017 | Significant |
| A-pH | 0.026667 | 1 | 0.026667 | 6.41 | 0.032 | |
| B- Amount of sorbent | 0.006667 | 1 | 0.006667 | 1.60 | 0.027 | |
| AB | 0.040000 | 1 | 0.040000 | 9.62 | 0.013 | |
| Lack of Fit | 0.029436 | 5 | 0.005887 | 2.94 | 0.159 | Not significant |
| Pure Error | 0.008000 | 4 | 0.002000 | - | - | |
| Core Total | 0.110769 | 12 | - | - | - | |
| R-Squared | - | - | 0.968312 | - | - | |
| Adj R-Squared | - | - | 0.953621 | - | - | |
| Std. Dev. | - | - | 0.017913 | - | - | |

## 3. Results and discussion
### 3.1. Characterization of adsorbent
#### 3.1.1. SEM and EDX analysis

SEM micrograph for the synthesized magnetic bentonite nanoparticles is represented in Fig. 2. It is clearly evident that the all these nanoparticles were well separated from each other suggesting the magnetic bentonite nanoparticles were free from aggregation and spherical. The SEM image of nanoparticles shows that the particles size ranged between 20 and 40 nm. The EDX spectrum (Fig. 3) contains intense peaks of O, Na, Mg, Al, Si, Ca and Fe. The atomic percentages obtained from EDX quantification (Table 4) were 69.02 % of O, 0.94 % of Na, 0.27 % of Mg, 3.69 % of Al, 11.04 % of Si, 0.25 % of Ca and 14.79 % of Fe. Presence of these elements on the surface of the nanoparticles indicate a large possibility of removal of diazinon.

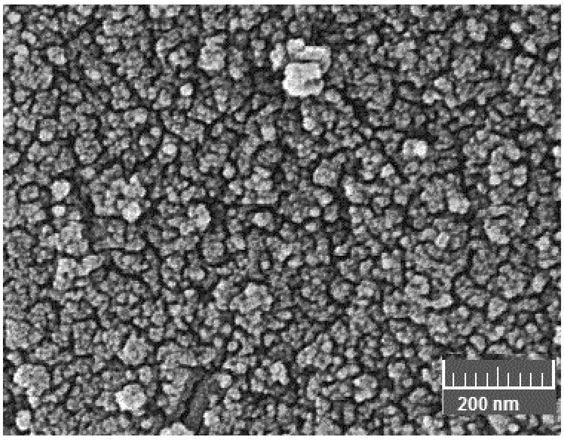


**Fig. 2.** SEM image of magnetic $Fe_3O_4$– bentonite nanoparticles on 200 nm scale.

**Table 4.** EDX spectrum obtained for magnetic bentonite.

| Elements | Weight, % | Atomic content, % |
|---|---|---|
| O | 46.43 | 69.02 |
| Na | 0.91 | 0.94 |
| Mg | 0.28 | 0.27 |
| Al | 4.19 | 3.69 |
| Si | 13.04 | 11.04 |
| Ca | 0.43 | 0.25 |
| Fe | 34.73 | 14.79 |
| Total | 100.00 | 100.00 |

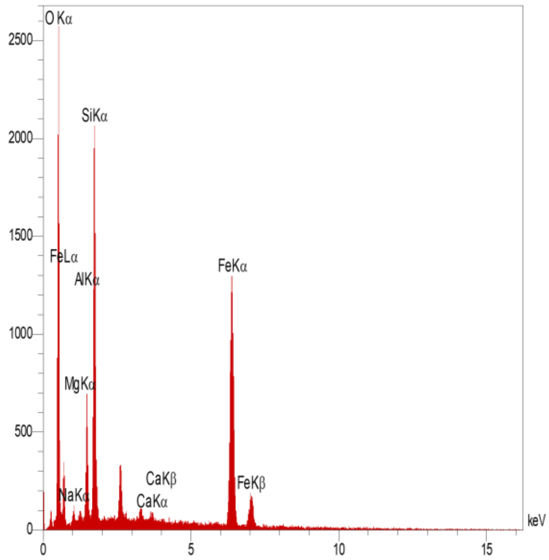


**Fig. 3.** EDX spectrum obtained for magnetic $Fe_3O_4$– bentonite nanoparticles.

#### 3.1.2. FTIR analysis

The binding properties of magnetic $Fe_3O_4$–bentonite nanoparticles were investigated by FTIR spectroscopic analysis and shown in Fig 4. The absorption broad band at 3629 $cm^{-1}$ was assigned to the hydroxyl (-OH) stretching vibrations of the Na-bent material surface. The absorption band at 3402 $cm^{-1}$ and 1630 $cm^{-1}$ displayed the presence of hydroxyl groups in the adsorbent. From the spectrum obtained, the peaks at 794, 1041 and 1088 $cm^{-1}$ are related to the stretching vibrations of Si–O groups, while the band at 916 $cm^{-1}$ was attributed to the stretching vibration of Al-O-(OH)-Al. Besides, the absorption bands at 520 and 469 $cm^{-1}$ are related to the presence of magnetic nanoparticles.

### 3.2. Plackett–Burman design for screening variables

From Fig. 5, the most significant variable on removal of diazinon is pH. Sorbent dosage is the next important factor, whereas contact time and agitation speed contribute non-significantly on the removal



Please cite this article as: S. Heydari, L. Zare, H. Ghiassi, Plackett–Burman experimental design for the removal of diazinon pesticide from aqueous system by magnetic bentonite nanocomposites, Journal of Applied Research in Water and Wastewater, 6 (1), 2019, 45-50.

efficiency of diazinon. Therefore, the pH level and sorbent dosage were selected in the optimization step.

### 3.3. Optimization using central composite design

In this study, central composite design (CCD) was utilized to determine the optimized levels of significant factors and investigate the interaction effects between main factors. The polynomial equation model to fit the removal efficiency of diazinon with the main factors were as follows:

R= -1.591 + 0.567 A + 33.3 B - 10.00 AB

where, R is the absorbance of sample; A is the reaction pH value and B is the sorbent dosage.

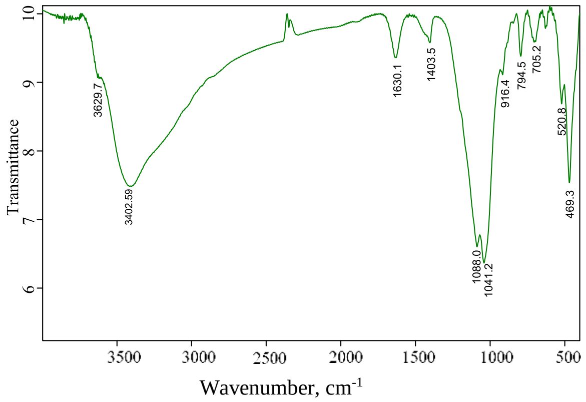


**Fig. 4.** FTIR spectrum of magnetic $Fe_3O_4$– bentonite nanoparticles.

The analysis of variance (ANOVA) of the optimization study showed that A, B, and interaction between A and B were significant ($p < 0.05$). To display the fitness of model, the lack of fit test was used. The results suggested that the lack of fit were non-significant, with high values for $R^2$ (0.9683) and adjusted $R^2$ (0.9536). The values of $R^2$ and adjusted $R^2$ of the quadratic regression model indicated that the model developed during this study satisfactorily predicted the removal of diazinon (Montgomery. 2007). Table 3 presented p-value of the variables included in the model. As the values of "Prob > F" less than 0.05, the model terms are significant. It can be concluded from Table 4 that two main variables, i.e. pH and the sorbent dosage, and the interactions between them are clearly significant. Also, according to the greater F-value (6.41), pH is the most important variable of the response.

Finally, the model was used to predict both the optimum value and optimum region of the factor level, which results in maximum. The statistical and perturbation plot analysis suggest that the optimized conditions for diazinon (contact time of 30 min, pH of 2, agitation speed of 500 rpm and adsorbent dose of 4 mg/mL) showed maximum removal of 92.50 % of pesticide. An experimental run was carried out using the optimum combination of factors and results were found and listed in Table 5. The results indicate a good agreement between the predicted and experimental response thereby confirms the high performance of the model.

The existence of the high degree of agreement between the removal efficiency predicted by the model and the experimental results indicates that the model could be used effectively for the optimization of the effects of the factors on the removal efficiency of diazinon from water.

### 3.4. Adsorption kinetics and isotherm study

To describe the isotherm data, Langmuir and Freundlich isotherm models are applied. The higher $R^2$ value of 0.9386 of the Freundlich model than the Langmuir model depicted a heterogeneous adsorption for diazinon. The sorption capacity of diazinon onto nanocomposite was calculated to be 277.8 mg/g. According to Dubinin–Radushkevich model, the mean free energy for adsorption of diazinon by biosorbent is found to be 0.13 Kj/mol. This presents that predominant mechanism of the adsorption of pesticide by biosorbent is likely physical sorption. Adsorption kinetic based on pseudo-second-order model displays the linear plot with a correlation coefficient ($R^2$ 0.9986). Therefore, pseudo-second-order kinetic model is appropriate for assessment of adsorption kinetic of diazinon on sorbent surface.

### 3.5. Removal of diazinon from real samples using magnetic bentonite nanocomposites

To verify the applicability of the developed methods, the removal of diazinon from industrial wastewater and groundwater samples were performed. All the samples were spiked with diazinon standard at $1\times10^{-2}$ mol/L; subsequently, the removal process was studied by standard addition method. Pesticide removal, in all the samples, was more than 89 % which reveals the effectiveness of this method for all samples.

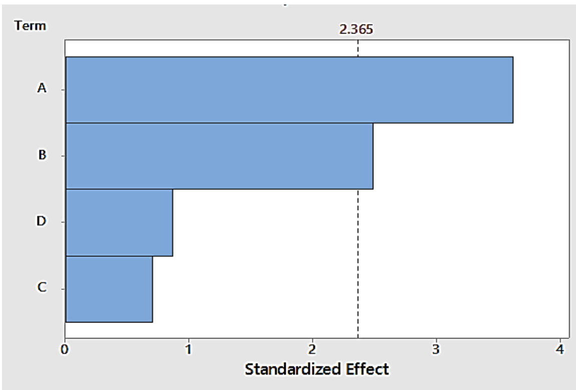


**Fig. 5.** Pareto chart of standardized main effect for Plackett–Burman design for diazinon (A: pH, B: sorbent dosage, C: agitation speed, D: contact time).

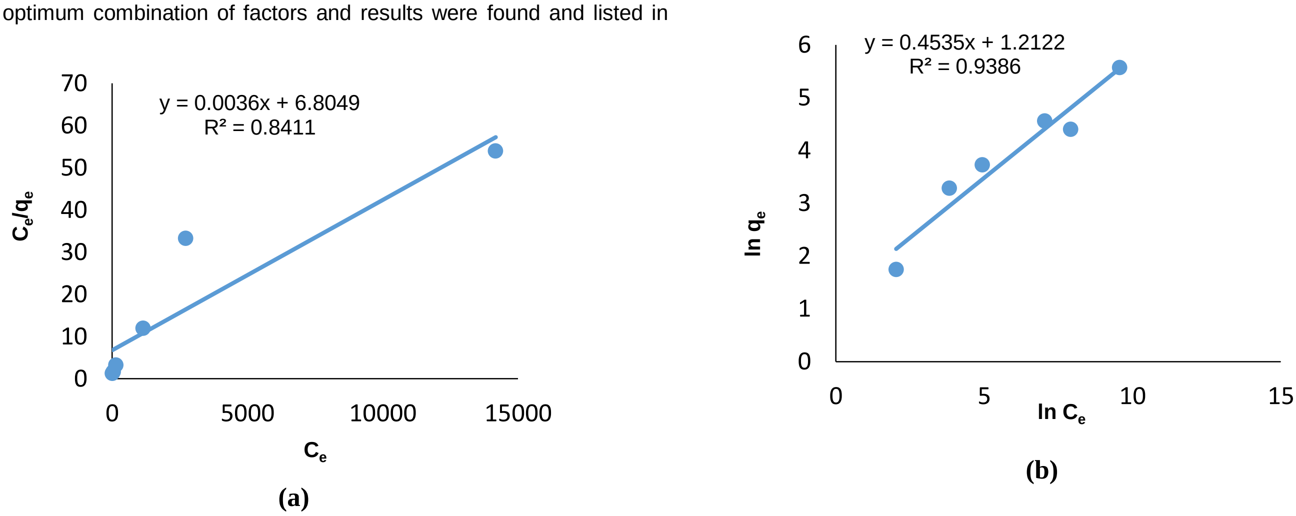


**Fig. 6.** (a) Langmuir plot, and (b) Freundlich plot for adsorption of diazinon on the sorbent.

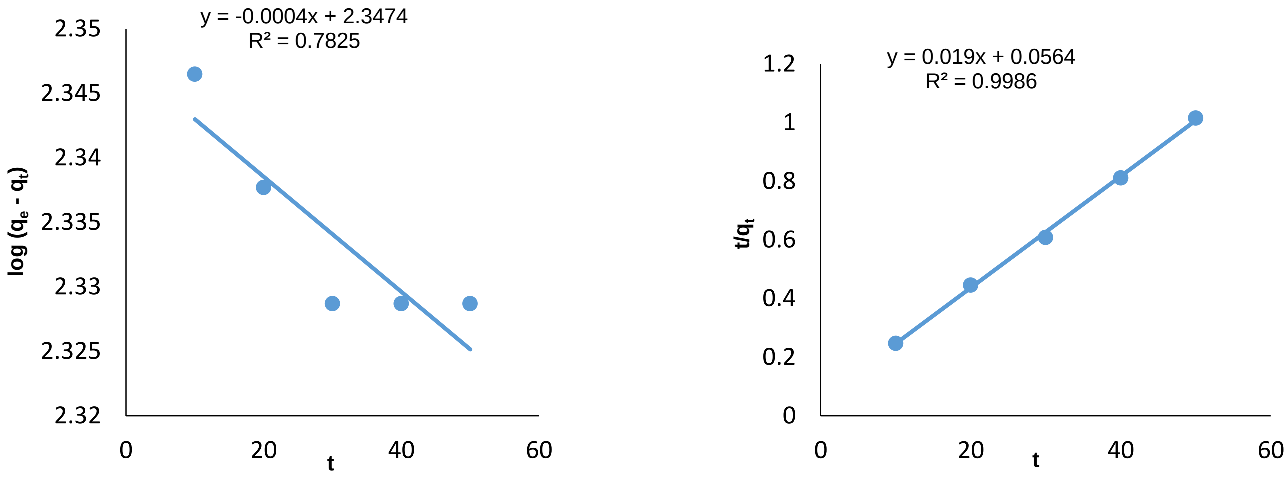


**Fig. 7.** (a) Pseudo-first-order, and (b) Pseudo-second-order kinetic plots for adsorption of diazinon on the sorbent.

**Table 5.** Optimization level of parameters.

| pH | Amount of sorbent (mg/ml) | Contact time (min) | Agitation speed | Response | |
|---|---|---|---|---|---|
| | | | | Predicted (%) | Experimental (%) |
| 2 | 4 | 30 | 500 | 92.50 | 90.61 ± 0.76 |

**Table 6.** Freundlich and Langmuir constants for adsorption of diazinon on magnetic bentonite.

| Freundlich constants | Value |
|---|---|
| $K_f$ (mg/g) | 3.3609 |
| n (L/g) | 2.2051 |
| $R^2$ | 0.9386 |
| **Langmuir constants** | **Value** |
| $q_m$ (mg/g) | 277.778 |
| b (l/g) | 0.0005 |
| $R^2$ | 0.8411 |

**Table 7.** Kinetic model parameters for adsorption of diazinon on magnetic bentonite.

| Pseudo-first order | Value |
|---|---|
| $q_e$ (mg/g) cal | 222.536 |
| $K_1$ (1/min) | 0.0009 |
| $R^2$ | 0.7825 |
| **Pseudo-second order** | **Value** |
| $q_e$ (mg/g) (cal) | 52.632 |
| $K_2$ (g/mg.min) | 0.0064 |
| $R^2$ | 0.9986 |

## 4. Conclusions

This work described the applicability of magnetic bentonite nanocomposites for diazinon removal. Under optimal values of process parameters, 92.50 % removal of pesticide was found. The results showed that Plackett–Burman design was an effective method to optimize the variables to increase the diazinon removal. The adsorption kinetics of pesticide was fitted to the pseudo-second order kinetic model. The higher $R^2$ value of 0.9386 of the Freundlich model than the Langmuir model depicted a heterogeneous chemisorption for diazinon. The sorption capacity of diazinon onto nanocomposite was calculated to be 277.778 mg/g. The mean free energy for adsorption of diazinon by sorbent was found to be 0.13 Kj/mol. This presented that predominant mechanism of the adsorption of pesticide by nanocomposite is likely physical biosorption. The method was successfully applied for the uptake of diazinon from industrial wastewater and groundwater samples.

**Acknowledgements**

The authors acknowledge the financial support of this work by University of Torbat-e jam, Torbat-e jam, Iran.

**References**

Ahmed M.J., and Theydan S.K., Microwave assisted preparation of microporous activated carbon from Sins seed pods for adsorption of metronidazole antibiotic, Chemical Engineering Journal 214 (2013) 310–318.

Amer M.W., Khalili F.L, Awwad A.M, Adsorption of lead, zinc and cadmium ions on polyphosphate modified kaolinite clay, Journal of Environmental Chemistry and Ecotoxicology 2 (2010) 1-8.

Bama K., and Sundrarajan M., Ag/$TiO_2$/bentonite nanocomposite for biological applications: Synthesis, characterization, antibacterial and cytotoxic investigations, Advanced Powder Technology 28 (2017) 2265-2280.

Czitrom V., One-factor-at-a-time versus designed experiments, The American Statistician 53 (1999) 126-131.

Degtyareva I.A., Ezhkova A.M., Yapparov A.Kh., Yapparov I.A., Ezhkov V.O., Babynin E.V., Davletshina A.Ya., Motina T.Yu., Yapparov D.A., Production of nano-bentonite and the study of its effect on mutagenesis in bacteria Salmonella typhimurium, Nanotechnologies in Russia 11 (2016) 663–670.

Ehrampoush M.H., Sadeghi A., Ghaneian M.T., Bonyadi Z., Optimization of diazinon biodegradation from aqueous solutions by Saccharomyces cerevisiae using response surface methodology, AMB Express 7 (2017) 68-73.

Hassan A.F., Elhadidy H., Abdel-Mohsen A.M., Adsorption and photocatalytic detoxification of diazinon using iron and nanotitania modified activated carbons, Journal of the Taiwan Institute of Chemical Engineers 75 (2017) 299-306.

Ho Y.S., and McKay G., Sorption of dye from aqueous solution by peat, Chemical Engineering Journal 70 (1998) 115-124.

Huang Z., Li Y., Chen W., Shi J., Zhang N., Wang X., Li Z., Gao L., Zhang Y., Modified bentonite adsorption of organic pollutants of dye wastewater, Materials Chemistry and Physics 202 (2017) 266-276.

Jiang L., Ye Q., Chen J., Chen Z., Gu Y., Preparation of magnetically recoverable bentonite–$Fe_3O_4$–$MnO_2$ composite particles for Cd(II) removal from aqueous solutions, Journal of Colloid and Interface Science 513 (2018) 748-759.

Kabwadza-Corner P., Matsue N., Johan E., Henmi T., Mechanism of Diazinon Adsorption on Iron Modified Montmorillonite, American Journal of Analytical Chemistry 5 (2014) 70-76.

Lagergren S., About the theory of so-called adsorption of soluble substances, Kungliga Svenska Vetenskapsakademiens Handlingar 24 (1898) 1-39.

Lou Z., Zhou Z., Zhang W., Zhang X., Hu X., Liu P., Zhang H., Magnetized bentonite by $Fe_3O_4$ nanoparticles treated as adsorbent for methylene blue removal from aqueous solution: Synthesis, characterization, mechanism, kinetics and regeneration, Journal of the Taiwan Institute of Chemical Engineers 49 (2015) 199–205.

Luo X., Lei X., Xie X., Yu B., Cai N., Yu F., Adsorptive removal of Lead from water by the effective and reusable magnetic cellulose nanocomposite beads entrapping activated bentonite, Carbohydrate Polymers 151 (2016) 640-648.

Mahadevan H., Dev V.V., Krishnan K.A, Abraham A, Ershana O.C, Optimization of retention of phosphate species onto a novel bentonite-alum adsorbent system, Environmental Technology and Innovation 9 (2018) 1-15.

Martinez J. M., Volzone C., Garrido L.B., Evaluation of polymeric Al-modified bentonite for its potential application as ceramic coating, Applied Clay Science 149 (2017) 20-27.

Mehdinia A., Jebeliyan M., Kayyal T.B., Jabbari A., Rattle-type $Fe_3O_4$@$SnO_2$ core-shell nanoparticles for dispersive solid-phase extraction of mercury ions, Microchimica Acta 184 (2017) 707-713.

Montgomery DC, Introduction to statistical quality control: John Wiley & Sons (2007).

Motawie A.M., Madany M.M., El-Dakrory A.Z., Osman H.M., Ismail E.A., Badr M.M., El-Komy D.A., Abulyazied D.E., Physico-chemical characteristics of nano-organo bentonite prepared using different organo-modifiers, Egyptian Journal of Petroleum 23 (2014) 331-338.

Moussavi G., Hosseini H., Alahabadi A., The investigation of diazinon pesticide removal from contaminated water by adsorption onto $NH_4Cl$-induced activated carbon, Chemical Engineering Journal 214 (2013) 172-179.

Pandey S., A comprehensive review on recent developments in bentonite-based materials used as adsorbents for waste water treatment, Journal of Molecular Liquids 241 (2017) 1091-1113.

Polo M., Llompart M., Garcia-Jares C., Cela R., Multivariate optimization of a solid-phase microextraction method for the analysis of phthalate esters in environmental waters, Journal of Chromatography A 1072 (2005) 63-72.

Raushel F.M., Bacterial detoxification of organophosphate nerve agents, Current Opinion in Microbiology 5 (2002) 288-295.

Shah F., Kazi T.G., Naeemullah, Afridi H.I., Soylak M., Temperature controlled ionic liquid-dispersive liquid phase microextraction for determination of trace lead level in blood samples prior to analysis by flame atomic absorption spectrometry with multivariate optimization, Microchemical Journal 101 (2012) 5-10.

Sogorb M.A., Villanova E., Enzymes involved in the detoxification of organophosphorus, carbamate and pyrethroid insecticides through hydrolysis, Toxicology Letters 128 (2002) 215-228.

Sousa E.T., Rodrigues F.M., Martins C.C., de Oliveira F.S., Pereira P.A.P., de Andrade J.B., Multivariate optimization and HS-SPME/GC-MS analysis of VOCs in red, yellow and purple varieties of Capsicum chinense sp. Peppers, Microchemical Journal 82 (2006) 142-149.

Sulaymon A.H., Mohammed A.A., Al-Musawi T.J., Comparative study of removal of cadmium (II) and chromium (III) ions from aqueous solution using low-cost biosorbent, International Journal of Chemical Reactor Engineering 12 (2014) 1–10.

Turabik M., Gozmen B., Removal of basic textile dyes in single and multi-dyeso-lutionsby adsorption: statistical optimization and equilibrium isotherm studies, Clean-Soil Air Water 41 (2013) 1080–92.

Yeddou Mezenner N., Lagha H., Kais H., Trari M., Biosorption of diazinon by a pre-treated alimentary industrial waste: equilibrium and kinetic modeling, Applied Water Science 7 (2017) 4067–4076.



Please cite this article as: S. Heydari, L. Zare, H. Ghiassi, Plackett–Burman experimental design for the removal of diazinon pesticide from aqueous system by magnetic bentonite nanocomposites, Journal of Applied Research in Water and Wastewater, 6 (1), 2019, 45-50.